Supporting Information

Authors:

Fan Zhang, Fenyun Yi, Tao Meng, Aimei Gao, Dong Shu, Hongyu Chen, Honghong Cheng, Xiaoping Zhou

Manuscript title:

In-Situ Supramolecular Self-Assembly Assisted Synthesis of $Li_4Ti_5O_{12}$-Carbon-Reduced Graphene Oxide Microspheres for Lithium-Ion Batteries

The supporting information includes 11 pages, 8 figures and 2 tables in total.

Supporting Information

In-Situ Supramolecular Self-Assembly Assisted Synthesis of $Li_4Ti_5O_{12}$-Carbon-Reduced Graphene Oxide Microspheres for Lithium-Ion Batteries

Fan Zhang[a], Fenyun Yi[a*], Tao Meng[a], Aimei Gao[a], Dong Shu[a,b,c*], Hongyu Chen[a], Honghong Cheng[a], Xiaoping Zhou[a]

[a.] School of Chemistry and Environment, South China Normal University, Guangzhou 510006, P. R. China

[b.] Guangzhou Key Laboratory of Materials for Energy Conversion and Storage, Guangzhou 510006, P. R. China

[c.] Base of Production, Education & Research on Energy Storage and Power Battery of Guangdong Higher Education Institutes, Guangzhou 510006, P. R. China

[*]Corresponding author. E-mail:
yifenyun@126.com (Fenyun Yi);
dshu@scnu.edu.cn (Dong Shu).

Material characterization

Powder X-ray diffraction (XRD) measurements were carried out on a Rigaku diffractometer by using Cu-Kα radiation (λ=1.5406 Å). Fourier transform infrared spectroscopy (FTIR) was recorded on a Nicolet 5700 FTIR spectrometer. The thermogravimetric (TG) measurement was carried out by a TGA Q500 analyzer under an air-flow with a heating rate of 8 ℃ min^{-1}. The microstructures of samples were investigated by a transmission electron microscope (TEM, JEM-2100). Scanning electron microscopy (SEM, JEOL SM-6360LV) was used to observe the morphology of the samples. The Raman spectra were collected from LabRAM HR Evolution

spectrophotometer (Jobin-Yvon) with a wavelength of 514.5 nm. The pore size characteristics and Brunauer-Emmett-Teller (BET) specific surface areas of samples were obtained by N_2 isotherm adsorption/desorption measurements using an Micromeritics ASAP 2020.

Electrochemical measurements

All the electrochemical measurements were carried out using standard coin-cells (CR 2032) assembled in an argon-filled glovebox. The working electrodes were prepared as follows. The active material, polyvinylidene fluoride (PVDF), carbon black were mixed at the mass ratio of 80:10:10 in N-methylpyrrolidone (NMP) solvent via vigorously stirring to form a uniform slurry. Then, the slurry was coated on a copper foil and dried under vacuum at 65 ℃ for 24 h. The typical loading of active material is about 1.75 mg cm^{-2}. The half-cells were assembled using a lithium foil as the counter electrode and a polypropylene film as the separator. The electrolyte was 1 mol L^{-1} $LiPF_6$ dissolved in a mixture of ethyl carbonate (EC) and dimethyl carbonate (DMC) in a volume ratio of 1: 1. Galvanostatical charge-discharge cycles were carried out on a LAND-CT2001A battery tester at different current densities in the voltage range of 1.0-2.5 V. The electrochemical impedance spectroscopy (EIS) and cyclic voltammetry (CV) curves were measured on an electrochemical workstation (CHI660E). The CV curves were carried out in the potential range of 1.0 to 2.5 V at different scan rates. The EIS were performed in the frequency range of 0.01-100 KHz with an AC signal amplitude of 5 mV.

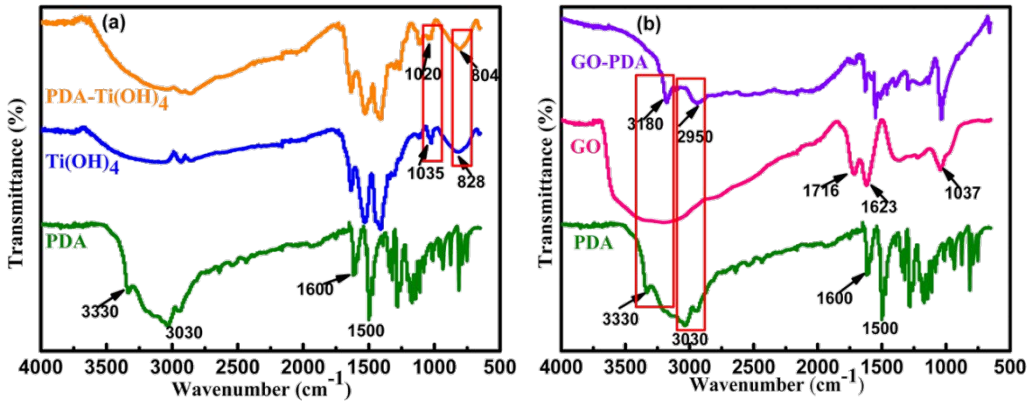

Fig. S1. FTIR spectra of (a) PDA-$Ti(OH)_4$, $Ti(OH)_4$, and PDA, (b) GO-PDA, GO, and PDA.

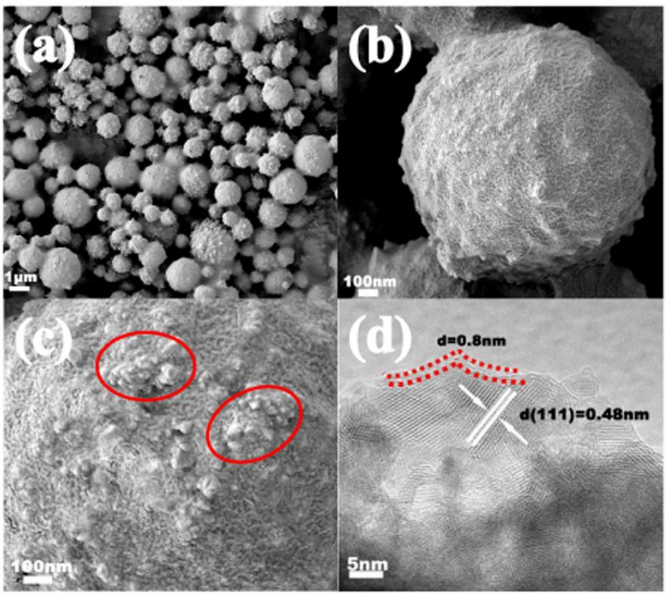

Fig. S2 SEM (a),(b),(c) images and HRTEM (d) of LTO-C.

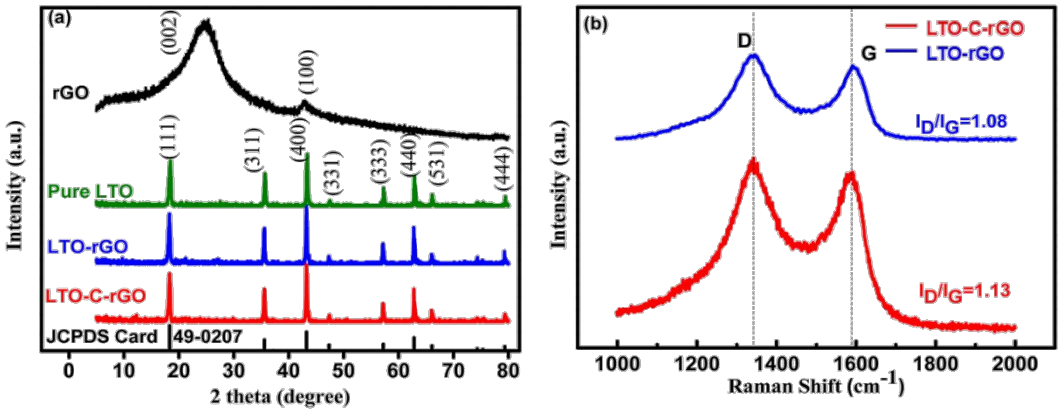

Fig. S3. (a) XRD patterns of rGO, LTO-C-rGO, LTO-rGO, and pure LTO. (b) Raman spectra of LTO-C-rGO and LTO-rGO.

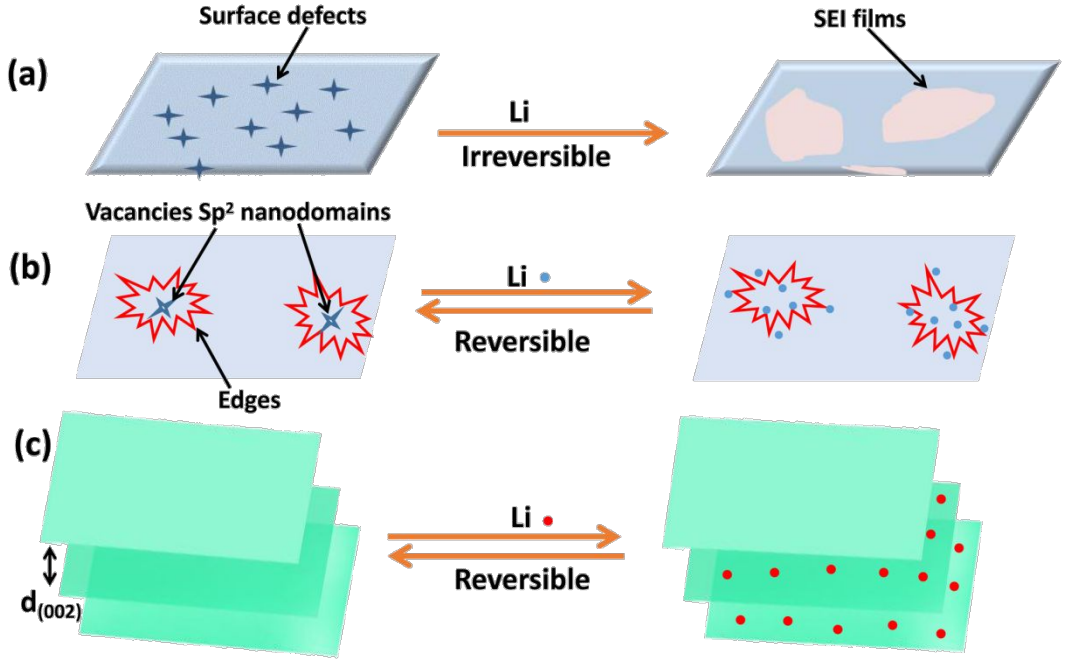

Fig. S4. (a) Irreversible Li storage at the interface between the graphene nanosheets and the electrolyte. (b) Reversible Li storage at the edge sites and the internal defects (e.g., vacancies) of nanodomains embedded in graphene nanosheets; (c) Reversible Li storage between (002) planes.[1-3]

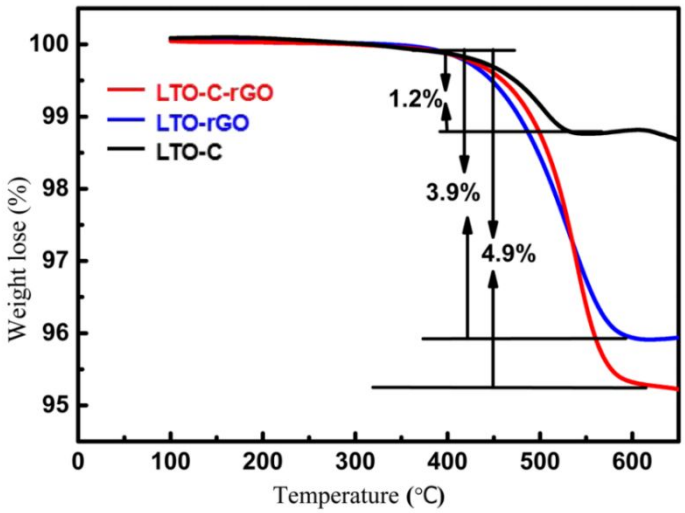

Fig. S5. TG profiles of LTO-C-rGO, LTO-rGO, and LTO-C

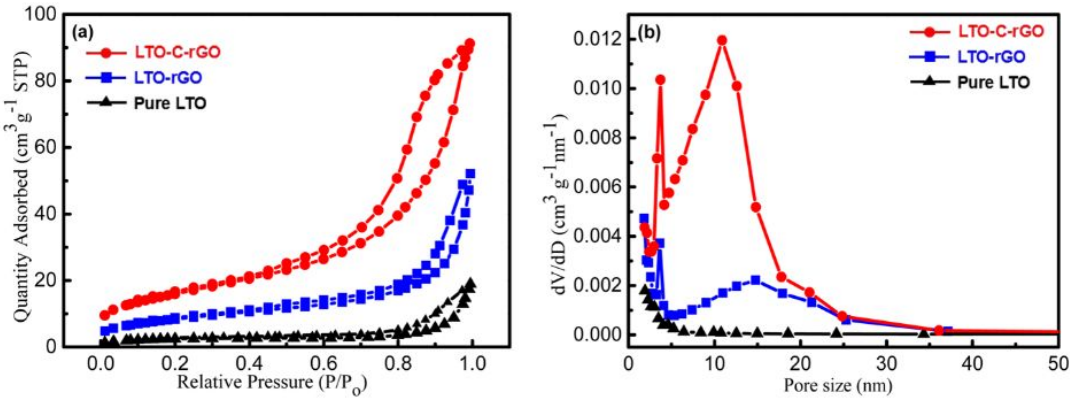

Fig. S6. (a) N_2 adsorption-desorption isotherm and (b) pore size distribution of pure LTO, LTO-rGO, and LTO-C-rGO.

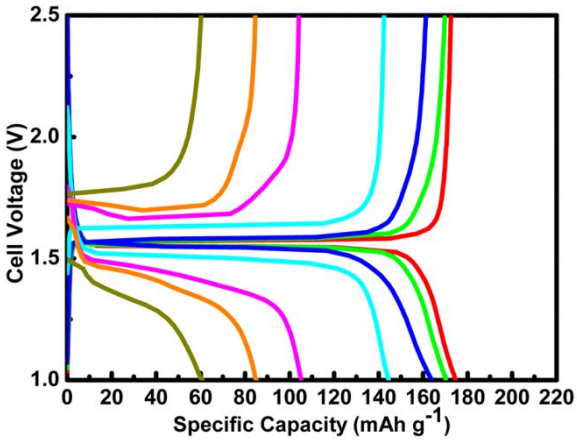

Fig. S7. Discharge/Charge curves of LTO-C electrode at different rates (from right to left): 0.1, 0.5, 1, 3, 5, 10, and 20 C.

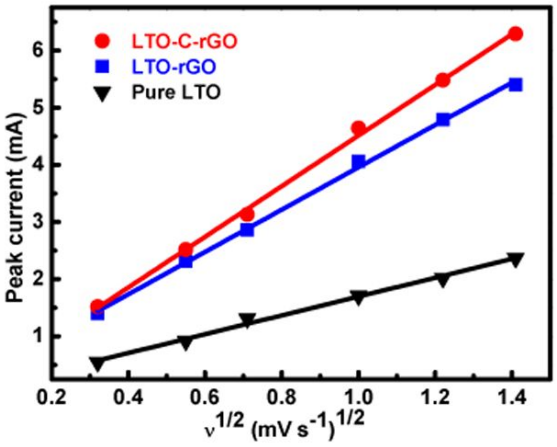

Fig. S8. The relationship plots between peak current and $\nu^{1/2}$.

Specific capacity for the graphene-based composite electrode material:[4]

$C_I = C_L \times \text{LTO wt.\%} + C_G \times \text{G wt.\%}$ (S1)

where C_I is the total specific capacity of the composite, C_L is the theoretical specific capacity of LTO, and C_G is the theoretical specific capacity of graphene. The theoretical specific capacities of LTO and graphene are 175 and 1100 mAh g^{-1}, respectively.

Calculation of Li+ diffusion coefficient (D_0) by CV test results

The peak current (i_p) is proportional to the square root of scan rate ($v^{1/2}$), which is expressed by the Randles-Sevcik equation (S1):[5]

$$i_p = (2.69 \times 10^5) n^{3/2} A D_0^{1/2} v^{1/2} C_0 \quad \text{(S2)}$$

In this equation, n is the number of electrons (=1 e^-) transferred in the Faradaic reaction, A is the surface area of the electrode (≈1.54 cm^2), D_0 is the Li^+ ion diffusion coefficient, v is the scan rate, and C_0 is the bulk concentration of Li^+ ions in the electrode (≈0.15 mol cm^{-3}).

Table S1. The performance comparison of the current LTO-C-rGO with previously reported LTO-based anodes:

Materials	Capacity retention	Rate performance	Ref
$Li_4Ti_5O_{12}$/graphene (1000:5)	about 77% after 500 cycle at 5 C	157 mA h g^{-1} at 1 C	6
$Li_4Ti_5O_{12}$/graphene	94.8% after 300 cycles at 20 C	171.7 mA h g^{-1} at 1 C	7
$Li_4Ti_5O_{12}$/graphene	89.8% after 100 cycles at 0.5 C	157.6 mA h g^{-1} at 1 C	8
$Li_4Ti_5O_{12}$ Coated with boron-doped carbon (3%)	90% after 200 cycles at 1 C	160 mA h g^{-1} at 1 C	9
Gd-doped $Li_4Ti_5O_{12}$	88% after 100 cycles at 10 C	150 mA h g^{-1} at 1 C	10
$Li_4Ti_5O_{12}$/rGO	95.4% after 100 cycles at 10 C	176.6 mA h g^{-1} at 1 C	11
$Li_4Ti_5O_{12}$/N-doped rGO	94.8% after 300 cycles at 10 C	152 mA h g^{-1} at 1 C	12
Li_2MoO_4 modified $Li_4Ti_5O_{12}$/C	92.5% after 200 cycles at 10 C	167.5 mA h g^{-1} at 1 C	13
$Li_4Ti_5O_{12}$/C/rGO	94.5% after 500 cycles and 97% after 300 cycles at 20 C	184 mA h g^{-1} at 1 C	This work

Table S2. EIS test results of pure LTO, LTO-rGO, and LTO-C-rGO sample

Samples	R_s/Ω	R_{ct}/Ω	σ /Ω•cm^2•$s^{-1/2}$	D/ cm^2•s^{-1}
pure LTO	11.22	31.23	27.41	1.04×10^{-12}
LTO-rGO	11.02	14.29	13.68	4.17×10^{-12}
LTO-C-rGO	11.24	9.01	8.49	1.08×10^{-11}

Calculation of Li^+ diffusion coefficient (D) by EIS test results

According to the following equation., the diffusion coefficient (D) of Li^+ can be calculated.[13-14]

$$D = \frac{R^2T^2}{2A^2n^4F^4C_{Li}^2\sigma^2} \quad \text{(S3)}$$

where R is the gas constant, T is the absolute temperature, A is the surface area of the anode, n is the number of electrons transferred in the half-reaction for the redox couple of Ti^{4+}/Ti^{3+}, F is the Faraday constant, C_{Li} is the molar concentration of Li^+, σ is the Warburg factor that can be derived from the following equation:

$$Z_{re} = R_s + R_{ct} + \sigma\omega^{-1/2} \quad \text{(S4)}$$

Z_{re} and $\omega^{-1/2}$ are in a straight line with a slope of σ, using which in equation (S3) the Li^+ diffusion coefficient (D) can be obtained.

Reference

(1) Pan, D.; Wang, S.; Zhao, B.; Wu, M.; Zhang, H.; Wang, Y.; Jiao, Z. Li storage properties of disordered graphene nanosheets. Chem. Mater. 2009, 21, 3136-3142.

(2) Menachem, C.; Peled, E.; Burstein, L.; Rosenberg, Y. Characterization of modified NG7 graphite as an improved anode for lithium-ion batteries. J. power sources 1997, 68, 277-282.

(3) Winter, M.; Besenhard, J. O.; Spahr, M. E.; Novak, P. Insertion electrode materials for rechargeable lithium batteries. Adv. Mater. 1998, 10, 725-763.

(4) Jeong, J. H.; Kim, M.-S.; Kim, Y.-H.; Roh, K. C.; Kim, K.-B. High-rate $Li_4Ti_5O_{12}$/N-doped reduced graphene oxide composite using cyanamide both as nanospacer and a nitrogen doping source. J. Power Sources 2016, 336, 376-384.

(5) Reyes Jiménez, A.; Klöpsch, R.; Wagner, R.; Rodehorst, U. C.; Kolek, M.;

Nölle, R.; Winter, M.; Placke, T. A step toward high-energy silicon-based thin film lithium ion batteries. ACS nano 2017, 11, 4731-4744.

(6) Liu, H.; Wen, G.; Bi, S.; Gao, P. Enhanced rate performance of nanosized $Li_4Ti_5O_{12}$/graphene composites as anode material by a solid state-assembly method. Electrochim. Acta 2015, 171, 114-120.

(7) Shi, Y.; Wen, L.; Li, F.; Cheng, H.-M. Nanosized $Li_4Ti_5O_{12}$/graphene hybrid materials with low polarization for high rate lithium ion batteries. J. Power Sources 2011, 196, 8610-8617.

(8) S.G. Ri, L. Zhan, Y. Wang, L. Zhou, J. Hu, H. Liu, $Li_4Ti_5O_{12}$/graphene nanostructure for lithium storage with high-rate performance. Electrochim. Acta 2013, 109, 389-394.

(9) Su, X.; Huang, T.; Wang, Y.; Yu, A. Synthesis and electrochemical performance of nano-sized $Li_4Ti_5O_{12}$ coated with boron-doped carbon. Electrochim. Acta 2016, 196, 300-308.

(10) Zhang, Q.; Verde, M. G.; Seo, J. K.; Li, X.; Meng, Y. S. Structural and electrochemical properties of Gd-doped $Li_4Ti_5O_{12}$ as anode material with improved rate capability for lithium-ion batteries. J. Power Sources 2015, 280, 355-362.

(11) Meng, T.; Yi, F.; Cheng, H.; Hao, J.; Shu, D.; Zhao, S.; He, C.; Song, X.; Zhang, F. Preparation of lithium titanate/reduced graphene oxide composites with three-dimensional “fishnet-like” conductive structure via a gas-foaming method for high-rate lithium-ion batteries. ACS Appl. Mater. Interfaces 2017, 9, 42883-42892.

(12) Leng, K.; Zhang, F.; Zhang, L.; Zhang, T.; Wu, Y.; Lu, Y.; Huang, Y.; Chen, Y. Graphene-based Li-ion hybrid supercapacitors with ultrahigh performance. Nano Res. 2013, 6, 581-592.

(13) Liu, J.; Lin, Y.; Lu, T.; Du, C.; Wang, W.; Wang, S.; Tang, Z.; Qu, D.; Zhang, X. Characterization and electrochemical properties of Li_2MoO_4 modified $Li_4Ti_5O_{12}$/C anode material for lithium-ion batteries. Electrochim. Acta 2015, 170, 202-209.

(14) Abureden, S.; Hassan, F. M.; Lui, G.; Ahn, W.; Sy, S.; Yu, A.; Chen, Z. Multigrain electrospun nickel doped lithium titanate nanofibers with high power lithium ion storage. J. Mater. Chem. A 2016, 4, 12638-12647.